

## TECHNICAL NOTE

Shelley L. Smith,<sup>1</sup> Ph.D. and Gaylord S. Throckmorton,<sup>2</sup> Ph.D.

# A New Technique for Three-Dimensional Ultrasound Scanning of Facial Tissues\*

**ABSTRACT:** We report the development of an ultrasonic facial scanning technique that allows for the visualization of continuous contours without deforming surface tissues. Adhesive markers are placed on the face to enable measurement of facial tissue thicknesses at specific landmarks. The subject immerses the face in a clear plastic box filled with water for about 20 seconds while the researcher moves the transducer along the bottom of the box, guiding transducer movement by watching the facial image in a mirror placed below. 3D Echotech<sup>®</sup> software (1) builds the images from sequentially acquired 2D frames. Reliability of repeat measurements at landmarks is good, and individual tissues (skin, subcutaneous, muscle) can be distinguished. The method is simple, reliable, less expensive and less time consuming than alternatives such as magnetic resonance imaging (MRI). It is applicable in both research and clinical contexts.

**KEYWORDS:** forensic science, forensic anthropology, tissue thickness, tissue depth, facial reconstruction, craniofacial, surgery

Accurate measurements of facial tissue depths are useful for clinical, forensic, and basic research purposes. Facial tissue thicknesses have been measured from adult cadavers since the 1800s (2), and ultrasound has been employed for in vivo thickness measurement in several studies conducted in the past two decades (3–7). Ultrasound is both more convenient and less expensive than MRI or CT and is thus more applicable to routine clinical and research environments. However, the ultrasound technique of measuring tissue depths has involved visualization of discrete landmarks by placing a static transducer, loaded with abundant gel, directly over the landmark site. Because this technique employs direct surface contact it necessarily applies some pressure to the facial tissue and becomes problematic if the goal is to scan the continuous contour of the face, especially in areas of rapidly changing contour such as the oral and nasal regions. Current 3D ultrasound technology holds considerable promise for the visualization and measurement of facial tissues if the problem of tissue deformation can be resolved (8). To circumvent difficulties of tissue deformation during continuous three-dimensional scanning of facial tissues, we have developed a novel technique involving brief facial immersion in water.

<sup>1</sup> University of Texas at Arlington (Associate Professor, Anthropology) and Baylor College of Dentistry, Texas A&M (Adjunct Assistant Professor, Orthodontics).

<sup>2</sup> University of Texas Southwestern Medical Center (Professor, Cell Biology) and Baylor College of Dentistry, Texas A&M (Adjunct Professor, Orthodontics). Dallas, TX.

\* This research was supported in part by a Center Grant from the American Association of Orthodontics Foundation and the Center for Craniofacial Research and Diagnosis at Baylor College of Dentistry, Texas A&M University System Health Science Center.

Received 7 June 2003; and in revised form 19 Nov. 2003; accepted 19 Nov. 2003; published 7 April 2004.

## Materials and Methods

### *Subjects, Equipment, and Scanning Procedures*

Seven adult volunteers (4 males and 3 females) agreed to participate in this study to establish methods and reliability. The protocol for human subjects was approved by the IRB committees of the University of Texas at Arlington and the Baylor College of Dentistry.

Two scans of two individual points, two full sagittal scans, and two full lateral scans were obtained from each subject. All scans from each subject were collected on the same day. Subjects were first timed for 25 seconds without facial immersion to ensure that they could hold their breath for the requisite time. Although scanning is completed within 17 seconds, some time is required for the subject to get correctly positioned and become as still as possible before the scan begins. Scanning often can be completed in less than the fully allotted time, and healthy subjects do not experience difficulty. The skin surface is cleansed with an alcohol pad, and adhesive foil star markers (“Stickopotamus” brand) are placed at specific facial landmarks. These markers routinely create shadows but do not completely block the transmission of sound waves and so allow measurements to be made at or near the tagged sites. Figure 1 shows the placement of small star markers at landmarks for the sagittal scan.

Scans were acquired in two views, sagittal and lateral. A clear plastic box (44 × 44 × 15 cm) filled with water to a depth of 7 cm was used for sagittal scans. The box was positioned with the bottom edges placed securely on two small side tables, leaving the center of the bottom of the box exposed. A mirror was placed on the floor underneath the box and near the chair of the person conducting the scan. The researcher prepared the bottom of the plastic box by using the transducer to apply a layer of conducting gel (Aquasonic 100, Parker Labs, Inc., Fairfield, NJ) along the center of the exposed



FIG. 1—Subject with midsagittal markers at nasion (overlying conjunction of frontal and nasal bones), A-point (indentation below nose) and B-point (indentation of chin).

bottom surface of the box. For lateral scans a second, similarly positioned box ( $43 \times 90 \times 12$  cm) was filled to a depth of 5 cm. (If sagittal scans are collected after lateral scans, the longer box may simply be filled with additional water to avoid switching boxes.)

An Acoustic Imaging AI 5200 Ultrasound Imaging System was used with a flat-based 7.5 MHz transducer of 38 mm width. Focal zones and image settings were adjusted as needed. The FreeScan® Program designed by Echotech,® now distributed by GE Medical Systems (1), creates the 3D images. A device (the “PC Bird”) attaches to the transducer and to the computer to record, at 30 frames per second, the spatial position of the transducer in six degrees of freedom. Coordinates of the transducer are recorded via this magnetic field sensor as the transducer moves through the 17-second scan. After initial calibration of the system, a simple test-suite program run prior to data collection ensures that the sensor is functioning accurately.

For the sagittal scan, the standing subject takes a breath and leans forward to immerse his or her face in the water. Although exact positioning is not critical due to the ability of the software to track spatial location, the midline of the face needs to be positioned within the prepared line of gel along the bottom of the box and the chin and the forehead should be at approximately the same distance from the bottom of the box (i.e., the face should not be tilted up or down). The nose should be near, but not touching, the bottom of the box. The subject should attempt to maintain a relaxed facial expression (Fig. 2). When the subject is positioned and still, the researcher scans from the subject’s chin toward the forehead (i.e., toward the researcher) watching in the mirror for correct alignment. The transducer is kept perpendicular to the box, avoiding a loss of contact with the box, and is moved in a straight line, without deviating to the right or left. Upon completion, the subject gently dries his or her face, avoiding marker removal, and rests while the researcher reviews the scan to ensure that all markers are clearly visible, facial alignment is appropriate, and differentiation of tissues is clear.

For lateral scans, the subject places the left cheek in the water, with the nose generally out of the water to allow breathing. (Some subjects may choose to hold their breath.) For lateral views, straight scans without curves allow for more precise control of orientation of the probe. In our current research, we are collecting three straight

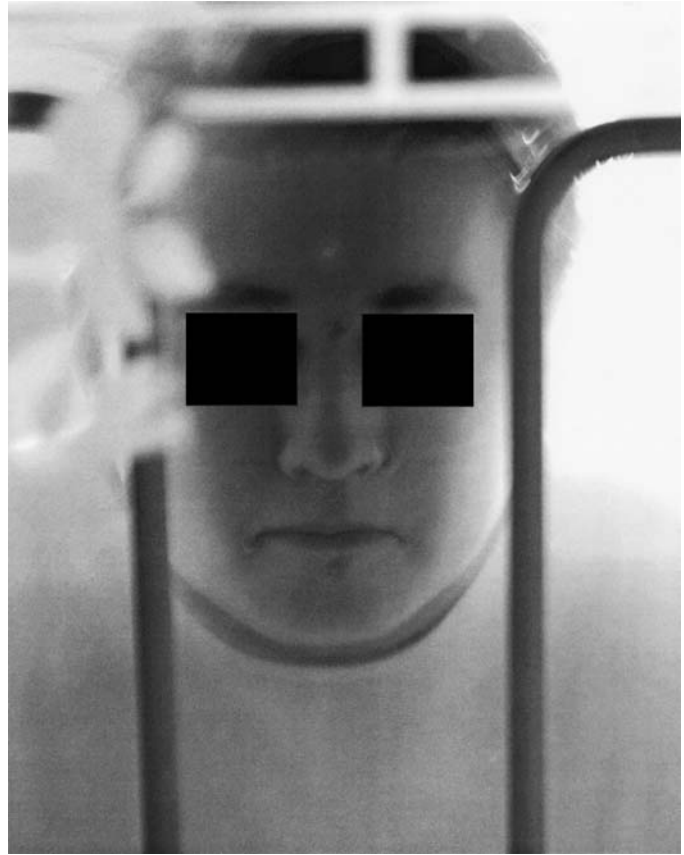


FIG. 2—Subject with face immersed in water, as viewed from the mirror below. The pattern evident in the upper left is from the mirror.



FIG. 3—Subject with lateral view markers. The anterior ramus (R) point is indicated by the arrow. Note bent corners of lateral view markers.

scans covering the landmarks shown in Fig. 3. Here we report data only for the anterior ramus (R) point from the single-point lateral scans. The marker for R-point is placed along the anterior edge of the mandibular ramus at approximately occlusal level.

*Postprocessing and Analysis of Data*—3D Echotech® software contains a variety of utilities for processing the data. The scan area can be cropped, discarding areas outside the field of interest. Cropping speeds up subsequent processing of the data. The software

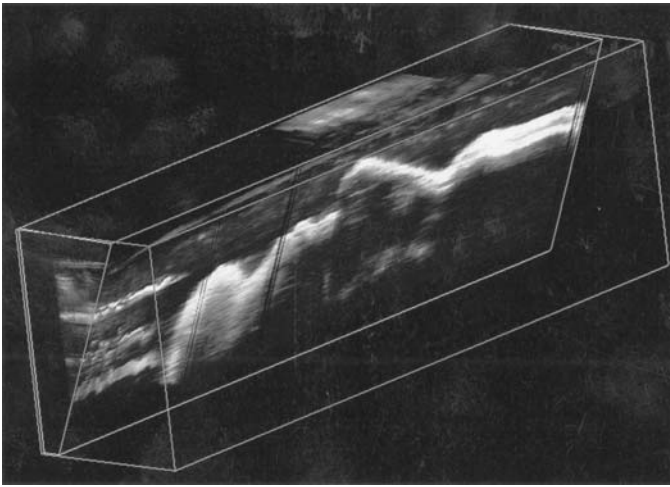


FIG. 4—Profile view of subject in “cube” constructed by Echotech® software. Note that it is necessary to create an oblique plane to obtain the profile for this subject.

creates 3D reconstructions of the images, eliminating artifacts due to changes in orientation of the ultrasound probe. It allows adjustment of the plane of section, ensuring that measured distances are perpendicular to the image surface. Additionally, one can display a 3D surface image that can be rotated to different orientations. A display setup window provides brightness and contrast scales that can be changed to optimize the visualization of tissue differences. A zoom function allows for enlargement of areas of interest. Using a cursor and mouse, one can measure multiple linear, area, and volume parameters.

Once data for each subject have been acquired, the researcher first crops the image, outlining the desired scan area throughout all the frames of the scan. Next the measurement distance is calibrated by selecting the appropriate scale in the image. During calibration it is helpful to maximize the image by selecting the full-screen window. 3D reconstructions (“cubes”) are then built by the software, incorporating all 2D scans. Either the mouse or the plus and minus keys allow one to move sequentially frame by frame through the 2D slices of a 3D reconstruction to locate skin surface markers or other areas of interest. Zooming in on the region of interest aids visualization and differentiation of tissues. Oblique planes can be defined as well (Fig. 4), and planes of section can be adjusted. Three-dimensional surface reconstructions (Figs. 5 and 6) can be built if desired in addition to the 3D reconstructions displayed in the cube views.

The measurements presented here were all taken from 2D slices, without use of oblique planes. Measurements from scans of individual B-points and R-points, and later from scans of four landmarks on full sagittal views, were made on two consecutive days, first from each subject’s first scan and then from the second set of scans. Points on different paired scans were measured on different days to prevent maintenance of a clear mental image of the location from the previous matched scan. An attempt was made to find a similar location in the two paired scans of each subject even if the precise landmark could not be visualized. No scans were eliminated due to image quality, forcing a choice of location for each measurement.

The four sagittal measurements were (a) maximum nose projection and soft tissue thicknesses at (b) B-point, (c) A-point, and (d) nasion. Providing an additional indication of reliability for B-point, the measurements from scans of B-point alone were taken

14 weeks prior to B-point measurements from the full sagittal scans. All measurements were collected by one researcher (SLS).

For B-point, thickness was the distance between the skin surface and the highest tooth surface. For A-point, thickness was the distance from the skin surface of the philtrum to the bone surface. Measurements were taken at a vertical (superior-inferior) level as close to the base of the nose as possible. It is necessary to find a slice in which bone or tooth is visible. While the measurement location should be close to the base of the nose, sometimes no clear bottom to the image can be seen; if so, it is necessary to back up frame by frame until one appears. For nasion, thickness was the distance from the skin surface to the nasal bone. For nose projection, a straight line was constructed across the bottom of the nostril(s) within the first 2D slice with a clearly visible tip of the nose; the projection was the distance from the nasal tip to this constructed line. For the anterior ramus depth (Fig. 7), thickness was the full distance from the skin surface to the bone.

Following Bland and Altman (9), an estimate of measurement error was obtained by calculating half the square of the absolute value of the difference between each pair of measurements, summing these values, dividing this result by the sample size (seven), and taking the square root of that value to give the within-subject standard deviation,  $\zeta_w$ . Following the same authors, we report the repeatability of each measurement as  $\sqrt{2} \times 1.96 \zeta_w$ . For 95% of paired measurements on the same subject, the difference between the two is expected to be less than this value.

## Results and Discussion

Measurements from the paired scans for individual B-points and R-points are given in Table 1. B-point skin markers were often difficult to see, but B-point could be determined from the anatomy in this region. Differences between paired B-point measurements ranged from 0.1 mm to 1.7 mm. For the ramus measurement, the difference between paired measurements ranged from 0.1 mm to 1.8 mm. In both cases, the average difference between measurement pairs was less than 1 mm.

Repeat measurements from the full sagittal scans appear in Table 2. The average difference for B-point was similar to that for the scans for this individual point. The full range of four B-point measurements, from the two repeat episodes 14 weeks apart, was somewhat larger than the within-trial difference, averaging 1.4 mm. The average differences for A-point and for nasion were less than 1 mm. The average nose projection difference between the two measurement trials was within 1.5 mm. As shown in Fig. 7 for R-point, individual tissue types can be distinguished.

TABLE 1—Repeat measurements for individual points (mm).\*

Subject	B1	B2	R1	R2	B1-B2	R1-R2
1	16.4	15.6	28.4	30.0	0.8	1.6
2	11.9	12.6	27.2	27.0	0.7	0.2
3	10.1	8.5	22.4	22.5	1.6	0.1
4	15.4	14.8	29.6	29.0	0.6	0.6
5	12.7	11.6	20.4	20.2	1.1	0.2
6	11.1	11.0	24.8	23.7	0.1	1.1
7	10.7	12.4	22.8	24.6	1.7	1.8
Average	12.61	12.36	25.09	25.29	0.94	0.80
SD	2.41	2.37	3.42	3.55	0.57	0.70
$\zeta_w$	...	...	...	...	0.76	0.73
Repeatability	...	...	...	...	2.12	2.02

\* B1 and B2, first and second measurements of B-point; R1 and R2, first and second measurements of R-point. See text for definitions of  $\zeta_w$  and repeatability.

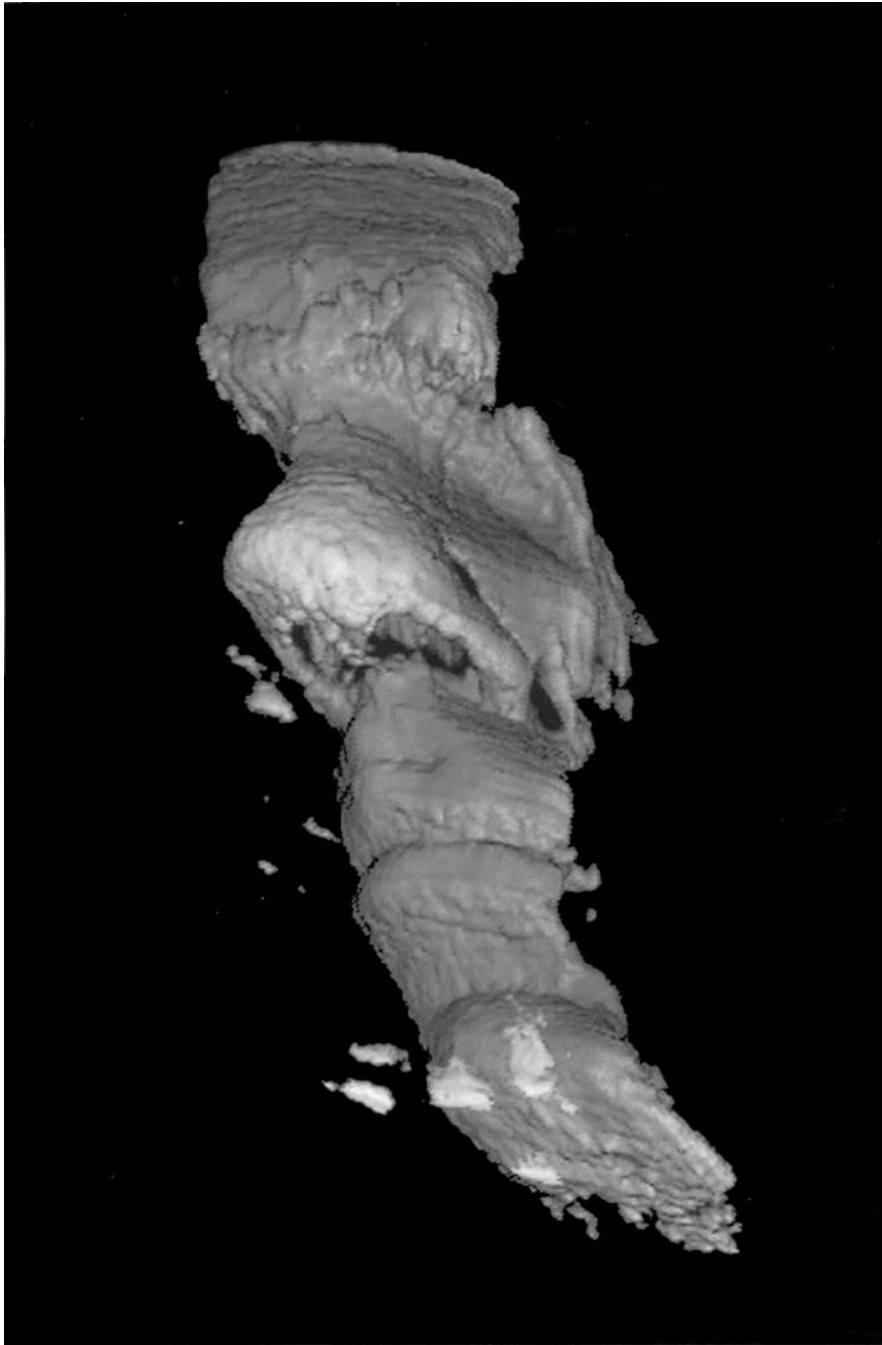


FIG. 5—3D surface reconstruction of a profile.

Reliabilities were generally good even though identical locations were not always available in paired scans for several reasons. Ideally points were measured from a visible skin marker to a clear surface (bone or teeth) below. However, in many instances skin markers were not clearly visible; in such cases the shadow created by the marker in the image sometimes served as a clue to marker location (Fig. 7). There is a trade-off between having a highly visible marker and a marker that does not obscure features of the image. The foil star markers generally work well but may at times be difficult or impossible to see and may come loose in the water or be removed by the subject in drying off and so require replacement. Given a visible marker, at times selecting a 2D slice or a measurement point some distance away from a marker was judged to allow a better measure-

ment. In addition, the 2D slice used for measurement must present reasonably clear top and bottom surfaces. Clear bottom surfaces were not visible in all views. Because the markers are visible over several frames, particularly in regions where the contour is changing rapidly and in locations on a sloping surface, small differences in location yield substantially different thickness measurements.

For the individual B-point scans, the two most discrepant pairs were from Subjects 3 and 7 (1.6 mm and 1.7 mm). For Subject 3, the incisor line was uneven; for Subject 7, the face was tilted in the water and no real B-point was visible. The largest paired difference for B-point from the full sagittal scans was 1.5 mm for Subject 4, who had a beard. Facial hair complicates location of the skin surface, so it is preferable that subjects be clean-shaven.

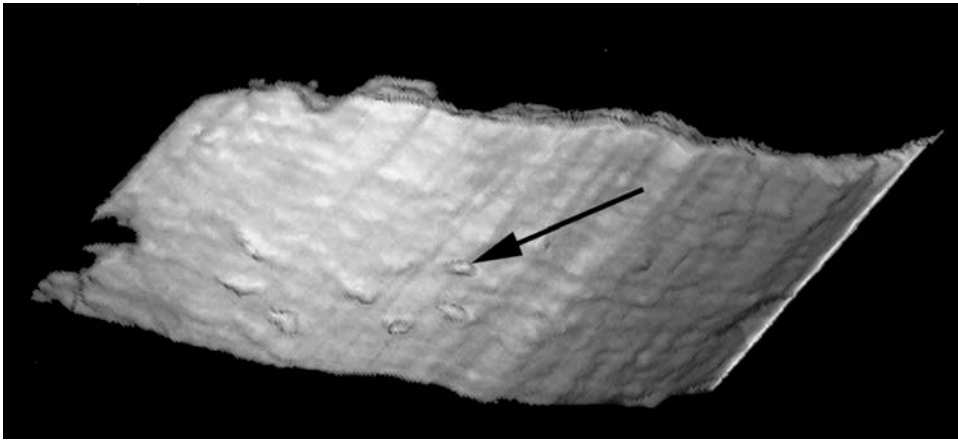


FIG. 6—3D surface reconstruction of a lateral scan. Note raised projections (arrow) from edges of lateral view markers.

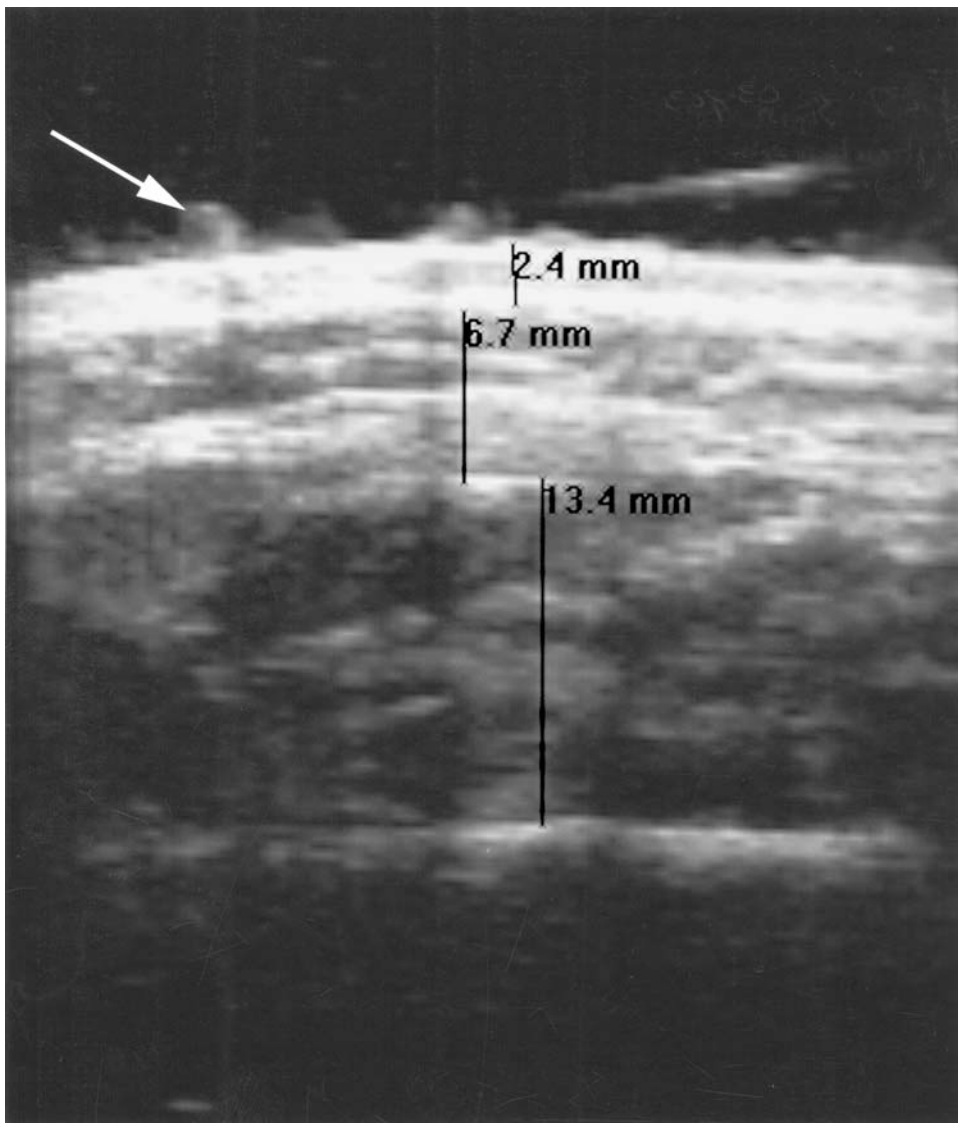


FIG. 7—Measurements from anterior ramus (R) point. Superficial skin tissue, subcutaneous tissue, and the masseter muscle can be distinguished. Arrow indicates raised projection of a lateral view marker.

TABLE 2—Repeat measurements from sagittal scans (mm).\*

Subject	B1	B2	A1	A2	NP1	NP2	NA1	NA2	B1-B2	A1-A2	NP1-NP2	NA1-NA2
1	16.0	15.1	17.4	16.7	30.1	32.4	12.7	9.9	0.9	0.7	2.3	2.8
2	12.0	11.3	14.2	13.4	27.9	30.2	6.6	6.4	0.7	0.8	2.3	0.2
3	8.8	10.0	11.0	11.3	24.3	24.4	5.7	7.0	1.2	0.3	0.1	1.3
4	16.4	14.9	13.2	13.2	26.7	27.5	9.3	7.9	1.5	0.0	0.8	1.4
5	11.3	12.3	8.1	8.4	26.9	26.1	6.3	6.2	1.0	0.3	0.8	0.1
6	10.9	10.3	14.8	13.6	29.0	26.7	8.5	8.1	0.6	1.2	2.3	0.4
7	11.1	11.1	10.2	12.0	20.5	18.8	4.9	4.5	0.0	1.8	1.7	0.4
Average	12.36	12.14	12.70	12.66	26.49	26.59	7.71	7.14	0.84	0.73	1.47	0.94
SD	2.81	2.09	3.14	2.53	3.22	4.35	2.68	1.71	0.48	0.62	0.90	0.97
$\zeta_w$	...	...	...	...	...	...	...	...	0.67	0.65	1.20	0.92
Repeatability	...	...	...	...	...	...	...	...	1.87	1.81	3.32	2.55

\* A = A-point; B = B-point; NA = nasion; NP = nose projection. First and second measurements of each point designated by 1 and 2, respectively, following lettered abbreviations. See text for definitions of  $\zeta_w$  and repeatability.

A-point results were generally good. The most discrepant pair (Subject 7) was affected by breaks in the image below the nose in the second scan. Such breaks result from too rapid movement of the probe.

The results for the nose projection measurement were not as good as anticipated. Although this should be a fairly simple measurement, the nasal tip must be clearly visible. If one must progress through frames superiorly to see the “tip,” a maximum length is not obtained because the distance progressively shortens superiorly. It is notable that for Subject 3, the only subject who wore a marker for the nasal tip, the repeat measurement was highly reliable (0.1 mm).

The results for nasion were predictably worse. The tissue is very thin in this location, so any significant measurement error yields poor reliability. In addition, it is difficult to locate the nasal bone and to distinguish this thin bone from other high-contrast structures in the image. For clear cases (Subjects 2 and 5), reliability was quite consistent, but the average difference between pairs of measurements was nearly 1 mm, which is problematic for a thickness that averages only 7 to 8 mm. Nonetheless, 1 mm is still a small absolute difference, and tissue thickness is expected to change to some extent at different vertical levels; even if a marker is visible, it appears in multiple frames, so it is not to be expected that the measurement will be taken from exactly the same vertical (superior-inferior) point.

The greatest virtue of this novel technique is simultaneously a liability in a classic replication study, namely that the images are continuous rather than discrete. Finding the “same” point on two scans is sometimes very difficult. While a “better” measurement or view might be obtained by creating an oblique plane, this further increases the variation in the technique of measurement. A pilot study incorporating use of oblique planes increased reliability for B-point but decreased reliability for R-point, so continued manipulation of oblique planes was not attempted.

Wilkinson (7) raises the issue of the effects of gravity and facial positioning on measured tissue depths. While the face is not vertical for our scans, gravity operates in the opposite direction than it does for an MRI or computerized tomography (CT) scan, since the subject’s face is in a prone rather than a supine position. However, buoyancy of facial tissues in water will reduce gravitational effects. While water pressure is a factor to consider, it should introduce less tissue distortion than applying a probe, particularly a moving one, directly to the skin surface. Due to the need to hold one’s breath, the technique is not suitable for young children, but older children and adolescents should be able to follow the necessary protocol. If the 6 mm pen employed by Wilkinson (7) instead of a wider

transducer were to be made compatible with the Echotech® software, it should be possible to obtain a narrow 3D band without much tissue deformation over smooth surfaces, but maneuvering over soft and strongly contoured regions, such as the lips, would remain problematic.

Beyond demonstrating comparability to previous ultrasonic and radiographic techniques of measurement, the long-term value of this methodology lies in its ability to generate continuous contours and to allow 3D views without radiation exposure and without the expense of MRI. In addition to forensic uses, the visualization and measurements obtainable with this technique can assist in treatment planning and assessment in dentistry and craniofacial surgery. This technique can be used in longitudinal studies to obtain repetitive scans of growing children and it is more suitable for large cross-sectional surveys than other 3D methods such as CT or MRI. More data are needed from a variety of racial/ethnic and geographic groups and from individuals of different ages and nutritional levels to explore changes with growth and evident variation in facial regions such as the cheek (6,7,10). Ultrasound, both 2D and 3D, is a valuable technology in the collection of such data.

Perhaps the most commonly displayed 3D ultrasound images are of fetal faces. The clarity of these images prompted development of our technique involving facial immersion. Since the probe is scanned over the bottom of a clear plastic box, tissues are not compressed, and the fluid-facial boundary is clearly defined. Adhesive markers can be placed at desired landmarks, and bending the markers’ corners aids visualization.

In summary, our development of this technique is still in the early stages. Results to date indicate considerable promise for this new methodology of facial scanning. Reliability for thickness measures is reasonably good, different tissue types are distinguishable, and tissue compression is avoided. The method is simple, relatively inexpensive, and applicable in both research and clinical contexts.

#### Acknowledgments

We thank the subjects who volunteered for this project for their patience and Tony Harris of GE Medical Systems for helpful technical advice. An anonymous reviewer drew our attention to references by Bland and Altman and provided good suggestions for improving clarity of presentation of results. Data were collected at Baylor in the lab of Dr. Peter H. Buschang, professor of orthodontics; we greatly appreciate the support and advice of Dr. Buschang throughout all phases of this project.

## References

1. Echotech. 3D FreeScan, Echotech 3D Imaging Systems. Operation Manual Version 6.0, Revision A. 2001.
2. Aulsebrook WA, İşcan MY, Slabbert JH, Becker P. [Superimposition and reconstruction in forensic facial identification: a survey](#). *Forensic Sci Int* 1995;75:101–20. [\[PubMed\]](#)
3. Hodson G, Lieberman LS, Wright P. *In vivo* measurements of facial tissue thicknesses in American Caucasoid children. *J Forensic Sci* 1985;30:1100–12. [\[PubMed\]](#)
4. Lebedinskaya GV, Balueva TS, Veselovskaya EV. Principles of facial reconstruction. In: İşcan MY, Helmer RP, editors. *Forensic analysis of the skull*. New York: Wiley-Liss, 1993;183–98. [\[PubMed\]](#)
5. Aulsebrook WA, Becker PJ, İşcan MY. [Facial soft-tissue thicknesses in the adult male Zulu](#). *Forensic Sci Int* 1996;79:83–102. [\[PubMed\]](#)
6. Manhein MH, Listi GA, Barsley RE, Musselman R, Barrow NE, Ubelaker DH. *In vivo* facial tissue depth measurements for children and adults. *J Forensic Sci* 2000;45:48–60.
7. Wilkinson CM. *In vivo* facial tissue depth measurements for White British children. *J Forensic Sci* 2002;47:459–65. [\[PubMed\]](#)
8. Nelson TR, Downey DB, Pretorius DH, Fenster A. *Three-dimensional ultrasound*. Philadelphia: Lippencott Williams and Wilkins, 1999.
9. Bland JM, Altman DG. Measurement error. *Brit Med J* 1996;312:1654. [\[PubMed\]](#)
10. Williamson MA, Nawrocki SP, Rathbun TA. Variation in midfacial tissue thickness of African-American children. *J Forensic Sci* 2002;47:25–31. [\[PubMed\]](#)

Additional information and reprint requests:  
 Shelley L. Smith, Ph.D.  
 Department of Sociology and Anthropology  
 Box 19599  
 University of Texas at Arlington  
 Arlington, TX 76019  
 E-mail: slsmith@uta.edu